

Deeply-Supervised CNN for Prostate Segmentation

Qikui Zhu
School of Computer
Wuhan University
WuHan, China,430079
Email: QikuiZhu@163.com

Bo Du
School of Computer
and State Key Lab of Information
Engineering on Survey,Mapping and Remote Sensing
Wuhan University
WuHan, China,430079
Email: gunspace@163.com

Baris Turkbey and Peter L . Choyke
National Cancer Institute
National Institutes of Health
9000 Rockville Pike, Bethesda, MD
Email: Ismail.Turkbey@nih.gov, pchoyke@mail.nih.gov

Pingkun Yan
Philips Research, 10 Center Driv, Bethesda
MD,20892,USA
Email: pingkun.yan@philips.com

Abstract—Prostate segmentation from Magnetic Resonance (MR) images plays an important role in image guided intervention. However, the lack of clear boundary specifically at the apex and base, and huge variation of shape and texture between the images from different patients make the task very challenging. To overcome these problems, in this paper, we propose a deeply supervised convolutional neural network (CNN) utilizing the convolutional information to accurately segment the prostate from MR images. The proposed model can effectively detect the prostate region with additional deeply supervised layers compared with other approaches. Since some information will be abandoned after convolution, it is necessary to pass the features extracted from early stages to later stages. The experimental results show that significant segmentation accuracy improvement has been achieved by our proposed method compared to other reported approaches.

I. INTRODUCTION

Over the past few years, the capabilities of Convolutional Neural Networks (CNNs) have achieved state-of-the-art performances in many fields, such as computer vision [1] and medical image analysis [2]. This success lies in the following aspects [3]: (1) more powerful graphics processing units (GPUs) have been developed; (2) a huge amount of available data, for example, about 1.2 million annotated images were provided in ImageNet Large Scale Visual Recognition Challenge (ILSVRC)¹. (3) Many networks have been designed for specific tasks, such as classification [4]–[6], segmentation [7], [8] and object detection [9], [10]. The core ability of CNNs is to learn hierarchical representation of the data, so adjusting networks' structure to improve the ability of hierarchical representation is a main objective in CNN based applications.

Classification is the most common application in CNNs, such as GoogLeNet [3], VGG-Net [9], where the output is a class label for the image. However, in many visual tasks, especially in medical image analysis [11], [12], specific needs

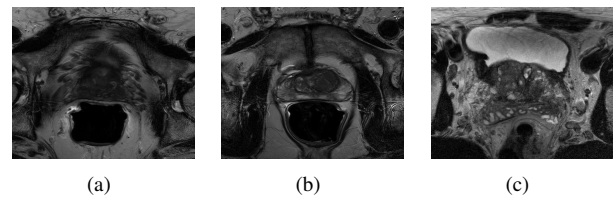


Fig. 1. Challenges in segmenting prostate in MR images. (a) Imaging artifacts inside the bladder. (b) Weak boundary. (c) Complex intensity distribution.

have to be met. For example, in medical image segmentation, the label is supposed to be assigned to each pixel and the result should have high precision. With impressive improvements by deep learning, more and more researchers apply these approaches in different medical image applications, such as image segmentation [8], [13], image fusion [14], image registration [15] and computer-aided diagnosis [16], [17].

Automatic segmentation is one of the pillars of medical image analysis. The key to segment medical images successfully is highly dependent on edge detection in a given context. So obtaining the edge's features and then searching for its position is the main work in many methods. Over the past decades, constructing effective feature engineering [18] has been a mainstream topic in medical image segmentation. For instances, Shen et al. [19] proposed the geometric moment invariant based features for feature-guided non-rigid image registration, and Liao et al. [20] proposed a representation learning method for automatic feature extraction in medical image analysis and a stacked dependent subspace analysis (ISA) deep learning framework is proposed to automatically learn the most informative features from the input image. Besides, shape-based models are widely used for image segmentation. Yan et al. [21] proposed a method of utilizing a prior shape estimated from partial contours for segmenting the prostate. Toth et al. [22] constructed an AAA model

¹<http://www.image-net.org/challenges/LSVRC/2014/>

by utilizing the intensity and gradient information, and then utilizing level-set method to segment prostate MRI. All of these methods segment the medical images by utilizing the specific features information. However, as we have described above, deep learning possesses good ability of learning hierarchical feature representations from data and has achieved record-breaking performance in a variety of applications. In terms of medical image analysis, which highly depends on edge detection. The main work in many methods is to find edges of the structure of interest. And deep learning can learn edge feature effectively. For instance, Xie and Tu [23] proposed a convolutional neural network based edge detection system for edge and object boundary detection. So we believe that deep learning can achieve great improvement in medical image analysis just like in computer vision. Many researchers have utilized deep learning in medical image analysis. For instances, Zhang et al. [8] proposed to use deep convolutional neural networks (CNNs) for segmenting isointense stage brain tissues using multi-modality MR images. Cheng et al. [24] proposed a supervised machine learning model which utilized atlas based Active Appearance Model and a deep learning model to segment the prostate on MR images. Chen et al. [25] proposed a deep contour-aware network that integrates multi-level contextual features to segment glands. All of these methods have utilized the advance of deep learning and obtained outstanding performances.

Many networks apply patch-to-pixel or patch-to-patch strategy to train and predict. However, this strategy always results in significantly downgraded training and prediction efficiency. The Fully Convolutional Neural networks (FCNs) [26] provide a way to train the network image-to-image, which allows us to train on a larger amount of samples simultaneously. However, we cannot directly apply FCN in prostate segmentation. Due to the prostate always lacks of clear boundary specifically at the apex and base, and the shape and texture are huge variation between different patients. These phenomena make the prostate segmentation become a challenge. Inspired by these methods and the superiority of deep learning, we propose a network which can forward the features extracted from early stages to later stages to avoid information lost. And to keep the features produced at hidden layers semantically meaningful, we put additional deeply supervised layers [27] at each stage. We name the proposed network as Deeply-Supervised CNN which, trained end-to-end, can segment the prostate prostate on MR images accurately and fast. Our network has three stages, the first stage consists of a compression path which extracts features from the data and reduce the resolution by an appropriate stride. The second stage of the network consists of an expansive path which upsamples the feature map and halve the number of feature channels until its original size is reached. In order to help the network learn more precise residual information, the third stage is constructed by deep supervised layers which supervise the process of training.

II. METHODS

A. U-Net

The architecture of U-Net [28] is illustrated in Fig 2. This contains two parts, the left part of the network is divided into four stages. Each stage consists of two convolutional layers and deals with different resolution feature maps. The convolution performed in left part uses 3x3 kernels, and each is followed by a rectified liner unit (ReLU) [29]. And at the end of each stage, a 2x2 max pooling operation with stride of 2 is attached for down sampling. The number of feature channels is doubled after each stage. The right part of the network is also divided into four stages. The architecture of the right part is similar to the left. Each stage of right part includes two kinds of operations. The first is upsampling which makes the size of feature map increase gradually until it reaches the size of the original input image. The second operation is to halve the number of feature channels, so that the number of convolution kernels will be halved after each stage. Since some image information will be lost after every convolution, it is necessary to put forward the features extracted from early stages of the left part to the right part. In order to achieve this function, the authors makes the left parts connected with the right parts. In this way, the network can gain some details that otherwise have been lost during convolution. And this operation will improve the quality of the final contour prediction. Besides these connections will speed up the convergence of the network.

B. Deeply-Supervised CNN

1) *Network Architecture:* In this section, we describe the details of the proposed network's architecture. As VGG-Net [9] has demonstrated that the representation depth is beneficial for classification accuracy. In order to obtain higher accuracy, it would be beneficial to utilize deeper network to segment prostate images. However, deeper network also brings two bottlenecks. First, deeper network typically means larger number of parameters, which make the network more prone to overfitting, especially for the application of medical images, because the number of labeled examples in the training set is always limited. The other bottleneck of deeper network is the dramatically increased use of computational resources. To solve this problem, we propose to use 1x1 convolutional layers in the convolutional process. The 1x1 convolution has two major advantages. On the one hand, they can reduce the dimensions and the number of parameters, remove computational bottlenecks to some extent; on the other hand, they can increase the depth of the network and improve the ability of character representation. In our network, we have applied 1x1 convolution in many stages to improve the accurate of segmentation.

As shown by GoogLeNet [3] that smaller convolutional kernels are more efficient in 2D network and smaller convolutional kernels can get the same effects as that large kernel gets. It can be proved that the effective receptive field size of stacked small kernels is equivalent to that of one large kernel.

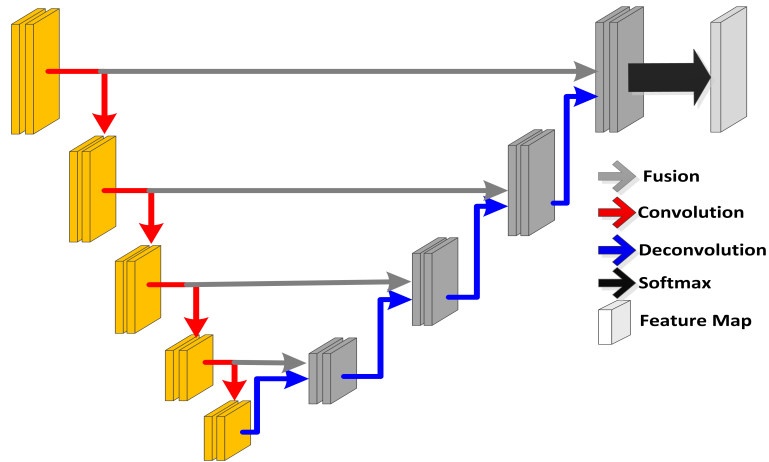


Fig. 2. U-net architecture. Each box corresponds to a multi-channel features maps. The number of features maps increases stage by stage on the left part. on the contrary, the number of features maps decreases stage by stage on the right part. The horizontal arrow denotes transfer residual information form early stage to later stage.

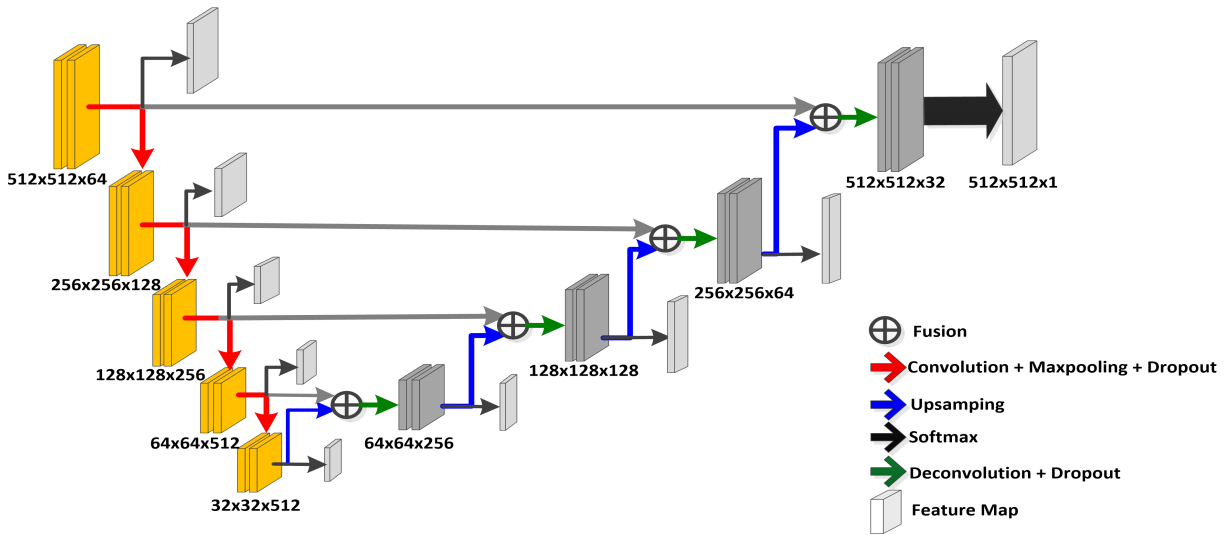


Fig. 3. Deeply-supervised CNN architecture. Each box corresponds to a multi-channel feature map. The number of feature map increase stage by stage on the left part. on the contrary, the number of feature map decrease stage by stage on the right part. The gray arrow denotes transfer residual information form early stage to later stage. At each stage, we add s supervised layer.

In addition, the smaller convolutional kernels can reduce the number of parameters and remove computational bottleneck simultaneously [3]. So in our network, the convolutional kernels size are all set as 3x3. Additionally, pooling operations have significance on improving the state-of-the-art convolutional networks and are useful to combat overfitting to some extent, so we have added pooling operations at the end of each stage.

As we have described above, the operation of convolution always results in image information lost. By forwarding the features extracted from early stages to later stages can provide those losing information for later stages. At last, improving the quality of final prediction. However, this is still leaves some space to be improved. When we forward features from early stages to later stages, due to lack of deep supervision, the features produced at hidden layers are less semantically meaningful. More importantly, they will significantly influence training and prediction efficiency. However, as Deeply-Supervised Nets [27] has demonstrated that deeply supervised layers can improve the directness and transparency of the hidden layer learning process. To overcome the described problems, we put eight additional deep supervised layers in the network. During training, all of these supervised layers supervise the process of training. Some times, since the depth of the network is large, the ability to propagate gradients back through all the layers in an effective manner is a concern. The additional supervised layers can solve the problem well by preserving gradients from early stage.

In summary, the proposed network contains three parts as shown in Fig 3. The first five stages consist of a compression path which extract features from the data and reduce the resolution by an appropriate stride. From top to the fourth stage, the number of feature channels is doubled at each stage. In the first stage, the number of feature channels is 64, for example, after four stages the number of feature channels increased to 512. In each stage, we perform two 3x3 convolutions, one 1x1 convolution and one 2x2 max pooling operation with stride 2 is attached for down sampling. On the contrary, the later four stages consist of an expansive path which upsample the features maps and halve the number of feature channels until its original size is reached. These stages have same operates like the stage within compression path except the max pooling operation. On the part of supervised layers, each supervised layer consists of a upsampling layer and a deconvolution layer. The upsampling layer upsamples the features map and then via deconvolution layer to obtain the segment result. During training, these supervised layers control the process of training according to the difference between segmentation result and ground truth .

The proposed network has some superiority over the original U-net. For instance, the 1x1 convolutions make the network become deeper as well as be not get into computational difficulties. And the operator of max pooling has significance in improving the state-of-the-art convolutional networks and overcoming the overfitting. Besides, the additional deep su-

pervised layers make the residual information meaningful and improve the convergence time of the model.

2) *Formulation:* We denote our input training dataset by $S = \{(X_n, Y_n), n = 1, \dots, N\}$, where $X_n = \{x_j^n, j = 1, \dots, |X_n|\}$ denotes the raw input image and $Y_n = \{y_j^n, j = 1, \dots, |X_n|\}$ denotes the corresponding ground truth binary edge map for image X_n . For simplicity, we denote all network layers' parameters as W . In deep supervised layers, the corresponding weights are denoted as $w = \{w^1, \dots, w^m\}$, where m denotes the number of deep supervised layers (in our method, $m=8$). We consider the objective function

$$L_{supervised}(W, w) = \sum_{i=1}^m \alpha_i l_{supervised}^i(W, w^i) \quad (1)$$

where $l_{supervised}$ denotes the image-level loss function for deep supervised layers' outputs. However, for the prostate images, the anatomy of interest occupies only a very small region of the scan. This always causes the network ignores the segmentation parts and the output of network are quite biased towards background, the learning process get trapped in local minima and can not obtain accurate results finally. To avoid this problem, in this paper, we utilized the dice coefficient as the objective function, which ranges between 0 and 1. The dice coefficient (DSC) [30] between two images can be written as

$$DSC(S_a, S_m) = \frac{2|S_a \cap S_m|}{|S_a| + |S_m|} \quad (2)$$

where S_a denotes the shape of automatic segmentation and S_m denotes the shape of manual segmentation.

In our work, the ground truth and result of segmentation are binary image, so the dice coefficient DSC between two binary images can be written as

$$DSC = \frac{2 \sum_i^N p_i q_i}{\sum_i^N p_i^2 + \sum_i^N q_i^2} \quad (3)$$

where N denotes the total number of pixels in the image, p_i and q_i denotes the pixel of ground truth and segmentation respectively.

Applying this formulation in our methods, we do not need to balance the number of samples between foreground and background pixels. Except for the supervised layers, we should also consider the final output. Putting all of loss together, we should minimize the following objective function via standard stochastic gradient descent

$$(W, w) = \operatorname{argmin}(L_{supervised}(W, w) + L(W, w)) \quad (4)$$

where $L(W, w)$ denotes loss function of the final output.

III. TRAINING

A. Dataset

In this work, all of the data is acquired from 81 patients. These images are acquired by a Philips 3T MRI scanner with endorectal coil. The in plane resolution is 0.3mm x 0.3mm and inter-plane distance is 3mm. Each volume consists of 26

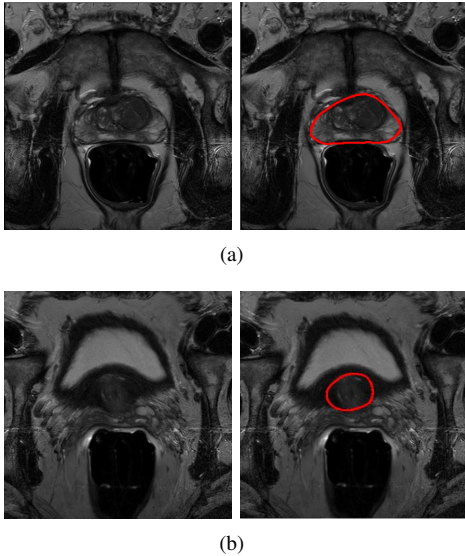


Fig. 4. Input image and the relative manual ground truth annotation.

slices and each slice has 512x512 pixels. When training the network, we remove some slices which do not contain the prostate. So, the total number of images is 1324.

The training and testing samples are randomly selected from the dataset. We selected 4 patients (totally 64 images) for testing and the rest of patients are utilized for training.

Since we have very limited number of images, it always results in the model suffering from overfitting. To increase the robustness and reduce overfitting, we employed the strategy of data augmentation to enlarge the training dataset. The augmentation transformations include translation, rotation and zoom.

B. Implementation Details

Our network is trained end-to-end on a dataset of prostate scans in MRI. All of the training images and ground truth have a fixed size of 512x512 and the framework is implemented under the open-source deep learning library Keras [31]. In the training phase, the learning rate is initially set as 0.001 and decreased by a weight decay. The momentum is 0.9, and due to the limitation of the memory, we choose 1 as the batch size. Experiments are carried out on GTX1080 GPU with 8 GB of video memory and the CUDA edition is 8.0.

IV. RESULT AND DISCUSSION

We trained our network on 77 patients. The input images and the manual ground truth annotation are shown in Fig.4. As we have described above, these images were acquired from different patients, and these images include the clinical variability. To evaluate our method, we randomly selected 4 patients with 64 images before training. These images do not take part in training and the prostate has been manually pre-delineated by a radiologist, which were used as the ground truth to evaluate the performance of automatic segmentation.

TABLE I
QUANTITATIVE COMPARISON BETWEEN THE PROPOSED APPROACH WITH OTHER METHODS

method	DSC		
	<i>meanDSC</i>	<i>medianDSC</i>	<i>maximumDSC</i>
<i>Our - model</i>	0.885	0.945	0.985
<i>U - Net</i>	0.865	0.940	0.969
<i>FCN</i>	0.759	0.832	0.918

We also selected dice coefficient as the evaluation method [30]. And to validate our method against U-Net and fully convolutional networks (FCNs), we used the same dataset to train and test the U-Net and FCNs.

1) *Qualitative Comparison:* To intuitively compare the proposed method with U-Net and FCN, the segmentation results of some representative and challenging samples are shown in Fig 5. It can be seen that these prostate images have fuzzy boundaries and the pixel intensity distributions are inhomogeneous both inside and outside of the prostate. Besides, both prostate and nonprostate regions have similar contrast and intensity distributions. All of these phenomenons make the segmentation difficult.

As shown in the second column in Fig 5. FCN model failed to obtain satisfactory result, though the model could detect part of prostate. However, for the details of prostate, for instance, the boundaries, the network can not assign the label to each pixel accurately.

In U-Net model, the label has been assigned to each pixel and has improved the segment accuracy as shown in the third column in Fig 5. However, the network always makes a mistake when assigning the label to nonprostate regions. Besides, for the boundaries information, the network cannot work well. At last, the segmentation results lose some important information and there still exist some errors.

The results of deeply supervised CNN are shown in the fourth column of Fig 5. The fuzzy boundaries are well detected by our proposed method. Besides, the segmentation boundary are more continuous and smooth than the competing method. It can be proved that additional supervised layers are useful for the texture and boundaries of prostate.

2) *Quantitative Comparison:* The statistical results of the three methods are shown in table I. We use three ways to evaluate the results. From table I we can see, the average of DSC values of our model, U-Net and FCN are 0.885, 0.865 and 0.759 respectively. Besides, all of the average, median and maximum DSC values of our method are the highest. So it can also be proved that the proposed method obtains significant improvement on the prostate segmentation compared with the other methods. These improvements can be attributed to the proposed network being more deeper and the additional supervised layers. During training, the additional supervised layers make a strong constraint on the network. And these supervised layers

can solve the problem that the fuzzy boundaries and the pixel intensity distributions are inhomogeneous both inside and outside of the prostate.

3) *Discussion*: Our results seem to yield a solid evidence that imposing a deeply supervised method during training the network is a viable method for improving neural network's performances for medical images segmentation. During training, all of these supervised layers will supervise the process of training and reduce the lose of prostate information. And due to the depth of the network's large scale, the additional supervised layers can provide gradients information for early stage which resolves the problem of gradients diffusion. As shown in Fig 6 . It can be seen that the different supervised layers can detect different textures. The later layers are closer to ground truth and the early supervised layers possess more information. So the supervised layers located in early stages could provide the information which was lost during training for the later stage.

V. CONCLUSION

In this paper, we propose a deeply-supervised CNN that utilized the residual information to accurately segment the prostate MRI. The proposed network is deeper and the number of parameters do not increase simultaneously compared with the traditional U-Net by applying 1x1 convolution. And the additional deep supervision plays a supervisory role during training the network. These supervised layers can avoid pixels' information loss to some extent during training. For the prostate image, the amount of background and foreground pixels are quite unbalanced. As a result, the network which ignores the segmentation parts and the output of network is strongly biased towards background. This result that the learning process get trapped in local minima and we can not obtain accurate results finally. To resolve this problem, we apply the dice coefficient as the objective function. The results show that the proposed network improves the performance of segmentation.

VI. ACKNOWLEDGEMENT

This work was supported in part by the Open Foundation of Basic Scientific Research Operating Expenses of Central-Level Public Academies and Institutes (CKWV2016380/KY), the National Natural Science Foundation of China under Grants 61471274 the Natural Science Foundation of Hubei Province under Grants 2014CFB193 and the Fundamental Research Funds for the Central Universities under Grants 2042016kf0152.

REFERENCES

- [1] H. Noh, S. Hong, and B. Han, "Learning deconvolution network for semantic segmentation," *Proceedings of the IEEE International Conference on Computer Vision*, vol. abs/1505.04366, 2015.
- [2] W. G. Baxt, "Use of an artificial neural network for the diagnosis of myocardial infarction." *Annals of Internal Medicine*, vol. 115, no. 11, pp. 843–8, 1992.
- [3] C. Szegedy, W. Liu, Y. Jia, and P. Sermanet, "Going deeper with convolutions," pp. 1–9, 2014.
- [4] A. Krizhevsky, I. Sutskever, and G. E. Hinton, "Imagenet classification with deep convolutional neural networks," *Advances in Neural Information Processing Systems*, vol. 25, no. 2, p. 2012, 2012.
- [5] K. Simonyan, A. Vedaldi, and A. Zisserman, "Deep inside convolutional networks: Visualising image classification models and saliency maps," *Computer Science*, 2014.
- [6] C. Dan, U. Meier, and J. Schmidhuber, "Multi-column deep neural networks for image classification," *Proceedings / CVPR, IEEE Computer Society Conference on Computer Vision and Pattern Recognition. IEEE Computer Society Conference on Computer Vision and Pattern Recognition*, vol. 157, no. 10, pp. 3642–3649, 2012.
- [7] S. E. a. D. T. Long, J., "Fully convolutional networks for semantic segmentation." In *Proceedings of the IEEE Conference on Computer Vision and Pattern Recognition*, pp. 3431–3440, 2015.
- [8] W. Zhang, R. Li, H. Deng, L. Wang, W. Lin, S. Ji, and D. Shen, "Deep convolutional neural networks for multi-modality isointense infant brain image segmentation." *Neuroimage*, vol. 108, pp. 214–224, 2015.
- [9] K. Simonyan and A. Zisserman, "Very deep convolutional networks for large-scale image recognition," *Computer Science*, 2014.
- [10] K. He, X. Zhang, S. Ren, and J. Sun, "Spatial pyramid pooling in deep convolutional networks for visual recognition." *IEEE Transactions on Pattern Analysis and Machine Intelligence*, vol. 37, no. 9, pp. 1904–16, 2014.
- [11] P. Yan, S. Xu, B. Turkbey, and J. Kruecker, "Adaptively learning local shape statistics for prostate segmentation in ultrasound." *IEEE Transactions on Biomedical Engineering*, vol. 58, no. 3, pp. 633–641, 2011.
- [12] C. C. Dan, A. Giusti, L. M. Gambardella, and Schmidhuber, "Deep neural networks segment neuronal membranes in electron microscopy images," *Advances in Neural Information Processing Systems*, vol. 25, pp. 2852–2860, 2012.
- [13] J. Kleesiek, G. Urban, A. Hubert, D. Schwarz, K. Maierhein, M. Bendzus, and A. Biller, "Deep mri brain extraction: A 3d convolutional neural network for skull stripping." *Neuroimage*, vol. 129, pp. 460–469, 2016.
- [14] H. I. Suk, S. W. Lee, and D. Shen, "Hierarchical feature representation and multimodal fusion with deep learning for ad/mci diagnosis." *Neuroimage*, vol. 101, pp. 569–582, 2014.
- [15] G. Wu, M. Kim, Q. Wang, B. C. Munsell, and D. Shen, "Scalable high-performance image registration framework by unsupervised deep feature representations learning." *IEEE Transactions on Biomedical Engineering*, vol. 63, no. 7, pp. 1–1, 2016.
- [16] D. C. Cirean, A. Giusti, L. M. Gambardella, and J. Schmidhuber, "Mitosis detection in breast cancer histology images with deep neural networks." in *Medical Image Computing and Computer-assisted Intervention: Miccai International Conference on Medical Image Computing and Computer-assisted Intervention*, 2013, pp. 411–8.
- [17] M. Drozdal, E. Vorontsov, G. Chartrand, S. Kadoury, and C. Pal, *The Importance of Skip Connections in Biomedical Image Segmentation*. Springer International Publishing, 2016.
- [18] L. Zhang, Q. Zhang, L. Zhang, D. Tao, X. Huang, and B. Du, "Ensemble manifold regularized sparse low-rank approximation for multiview feature embedding," *Pattern Recognit.*, vol. 48, no. 10, pp. 3102–3112, 2015.
- [19] D. Shen and C. Davatzikos, "Hammer: hierarchical attribute matching mechanism for elastic registration." *IEEE Transactions on Medical Imaging*, vol. 21, no. 11, pp. 29–36, 2001.
- [20] S. Liao, Y. Gao, A. Oto, and D. Shen, "Representation learning: a unified deep learning framework for automatic prostate mr segmentation." in *Medical Image Computing and Computer-assisted Intervention: Miccai International Conference on Medical Image Computing and Computer-assisted Intervention*, 2013, pp. 254–61.
- [21] P. Yan, S. Xu, B. Turkbey, and J. Kruecker, "Discrete deformable model guided by partial active shape model for trus image segmentation." *IEEE transactions on bio-medical engineering*, vol. 57, no. 5, pp. 1158–66, 2010.
- [22] R. Toth and A. Madabhushi, "Multifeature landmark-free active appearance models: Application to prostate mri segmentation," *IEEE Transactions on Medical Imaging*, vol. 31, no. 8, pp. 1638–50, 2012.
- [23] S. Xie and Z. Tu, "Holistically-nested edge detection," in *IEEE International Conference on Computer Vision*, 2015, pp. 1395–1403.
- [24] L. L. Cheng R, Roth H R, "Active appearance model and deep learning for more accurate prostate segmentation on mri." *International Society for Optics and Photonics*, vol. 100, pp. 978 421–978 421–9, 2016.
- [25] H. Chen, X. Qi, L. Yu, and P. A. Heng, "Dcan: Deep contour-aware networks for accurate gland segmentation," *arXiv:1604.02677*, 2016.

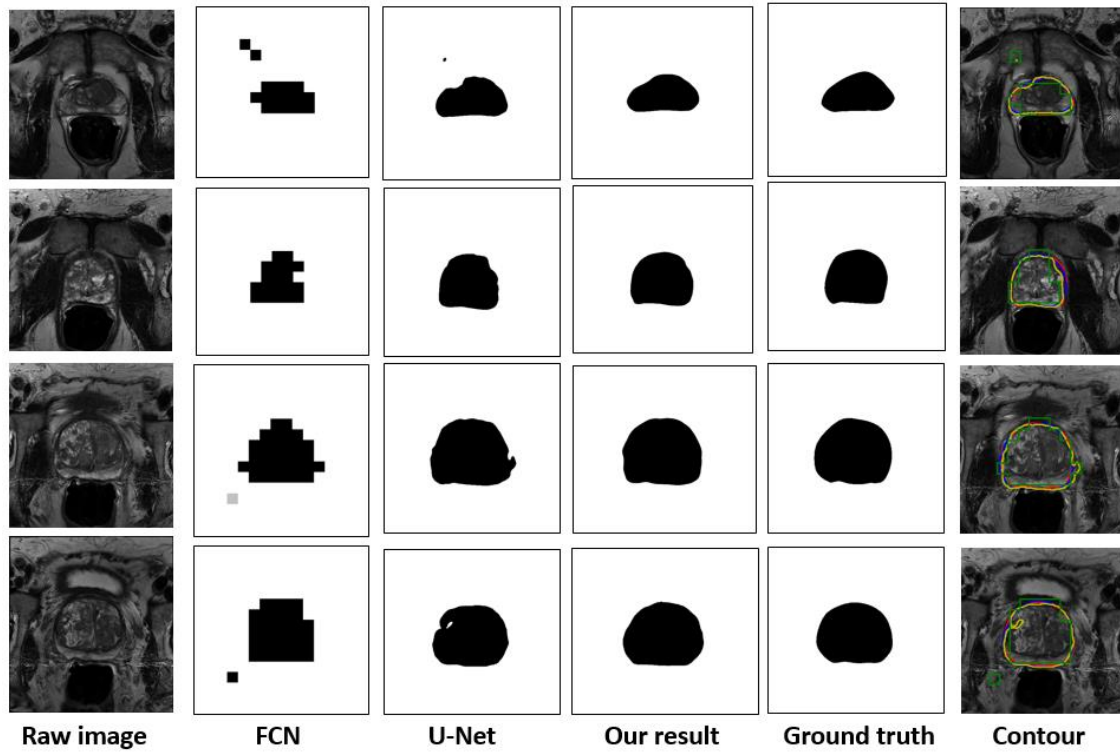


Fig. 5. Segmentation results. From left to right are Raw image,the segmentation results of FCN,the segmentation results of U-Net,the segmentation results of Deeply-supervised CNN, Ground Truth,Segmentation results respectively. The blue, red ,green and yellow contour denote ground truth, our result, the result of FCN and the result of U-Net respectively.

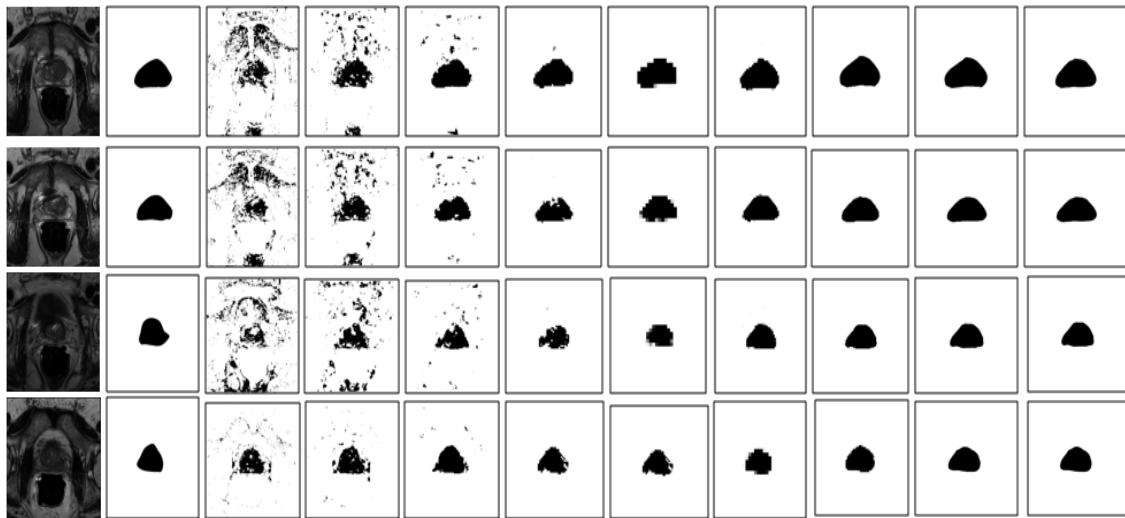


Fig. 6. Different deep supervised layers' segmentation results. From left to right are Raw image,Ground Truth,the segmentation results of deep supervised layers respectively.

- [26] J. Long, E. Shelhamer, and T. Darrell, "Fully convolutional networks for semantic segmentation," in *IEEE Conference on Computer Vision and Pattern Recognition*, 2015, pp. 1337–1342.
- [27] C. Y. Lee, S. Xie, P. Gallagher, Z. Zhang, and Z. Tu, "Deeply-supervised nets," *Eprint Arxiv*, pp. 562–570, 2014.
- [28] O. Ronneberger, P. Fischer, and T. Brox, "U-net: Convolutional networks for biomedical image segmentation," *International Conference on Medical Image Computing and Computer-Assisted Intervention*.
- [29] J. Gu, Z. Wang, J. Kuen, L. Ma, A. Shahroudy, B. Shuai, T. Liu, X. Wang, and G. Wang, "Recent advances in convolutional neural networks," *Computer Science*, 2015.
- [30] C. Duan, Z. Liang, S. Bao, and H. Zhu, "A coupled level set framework for bladder wall segmentation with application to mr cystography," *IEEE Transactions on Medical Imaging*, vol. 29, no. 3, pp. 903–915, 2010.
- [31] P. Charles, "Project title," *GitHub repository*, 2013.